Enhanced Electrogenerated Chemiluminescence of Phenylethynylpyrene Derivatives: Use of Weakly Electron-Donating Group as a Substituent

Yeon Ok Lee,[†,⊥] Tuhin Pradhan,[†,‡,⊥] Sangwook Yoo,[§,⊥] Tae Hyun Kim,[‖] Joohoon Kim,*[§] and Jong Seung Kim*[†]

[†]Department of Chemistry and [‡]Research Institute for Natural Sciences, Korea University, Seoul 136-701, Korea

[§]Department of Chemistry, Research Institute for Basic Sciences, Kyung Hee University, Seoul 130-701, Korea

[‖]Department of Chemistry, Soonchunghyang University, Asan 336-745, Korea

Ⓢ Supporting Information

ABSTRACT: A weakly donating group (*n*-propyl) has been used as a substituent at the *para*-position of the phenyl group for a series of phenylethynylpyrene derivatives where the number of phenylethynyl peripheral arms appended to the pyrene core is varied. This system markedly improved the concurrent stability of both cation and anion radicals and consequently greatly improved electrogenerated chemiluminescence (ECL). Density functional theory (DFT)-based theoretical calculations supported the associated photophysical and electrochemical properties of the series compounds.
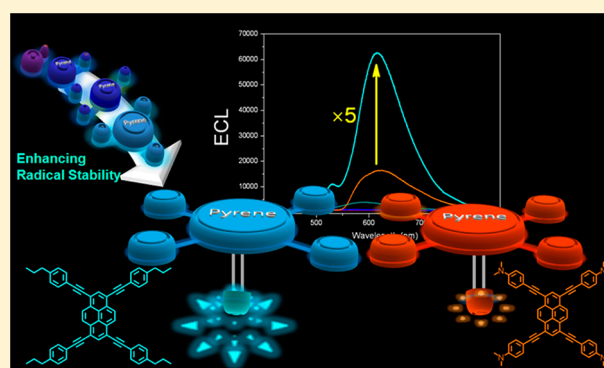
INTRODUCTION

Electrogenerated chemiluminescence (ECL), as a powerful analytical technique, is widely used for many purposes, such as immunoassays, DNA analyses, and molecular diagnosis of clinically important compounds (e.g., steroidal hormones, thyrotopin, digoxin, etc.), in combination with flow injection analysis (FIA), high-performance liquid chromatography (HPLC), capillary electrophoresis, and micro total analysis (μTAS).[1-4] ECL has also promising applications in OLEDs (organic light emitting diodes),[5] which are currently used in long-lived and highly efficient color displays. ECL is the process in which radical ions generated at electrodes undergo electron-transfer reactions to form excited states that emit light.[1] The generated radical ions are required to be stable enough to form emissive excited states and thus to exhibit a strong ECL because decomposition of the radical ions causes one of the redox processes to be chemically irreversible.[6,7] There have been efforts to enhance ECL efficiency by improving the radical stability.[6c,8] Bard et al. have improved the stability of radical cations generated from fluorene compounds for ECL enhancement by modifying the fluorene ring to 9,9′-spirobifluorene derivatives.[6c] In our previous study, we have also improved the radical cation stability of pyrene derivatives by increasing the number of peripheral donors appended to pyrene core.[8a] In this regard, we expect even greater ECL efficiency to be achieved if both the cation and anion radicals are concurrently made enough stable at the electrode surfaces. This is a very

challenging task especially for pyrene derivatives because increasing number of electron-donating groups in a compound not only enhances the cation radical stability but also reduces the anion radical stability, as we have observed in our previous work for tetrakis(ethynyl)pyrene series.[9] Similarly, the electron-withdrawing group enhances anion radical stability but also reduces cation radical stability at the same time.[9] Therefore, we require a judicial choice for the substituent group in order to achieve a balanced stability between cation and anion radicals simultaneously.

In this study, we prepared a series of phenylethynylpyrene derivatives using the *n*-propyl group as a substituent at the *para*-position of the phenyl group (**1−5**, Scheme 1). In comparison with our previous series,[8a] we replaced the dimethylamine ($-$NMe$_2$) group by the *n*-propyl group, which is a weakly electron-donating group, as to avoid the reciprocal relationship mentioned above in radical ions stability with a strongly electron-donating group. We have also varied the number of peripheral arms to verify and improve the stability of radical ions. We then performed the photophysical studies for the series to test the quantum efficiency and π-conjugated network in the molecules, the electrochemical studies to compare the radical stability, and finally the ECL studies. We also compared the ECL properties of the present series with the
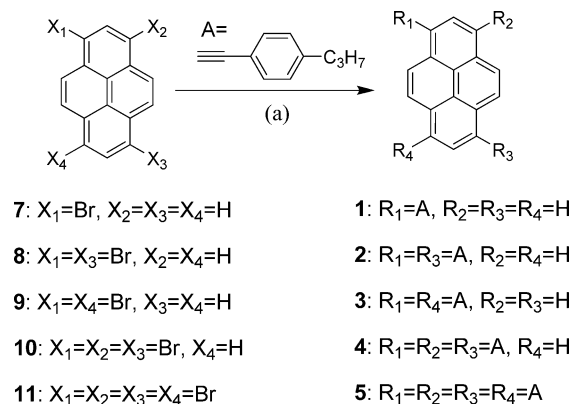
Scheme 1. Chemical Structures of 1−6
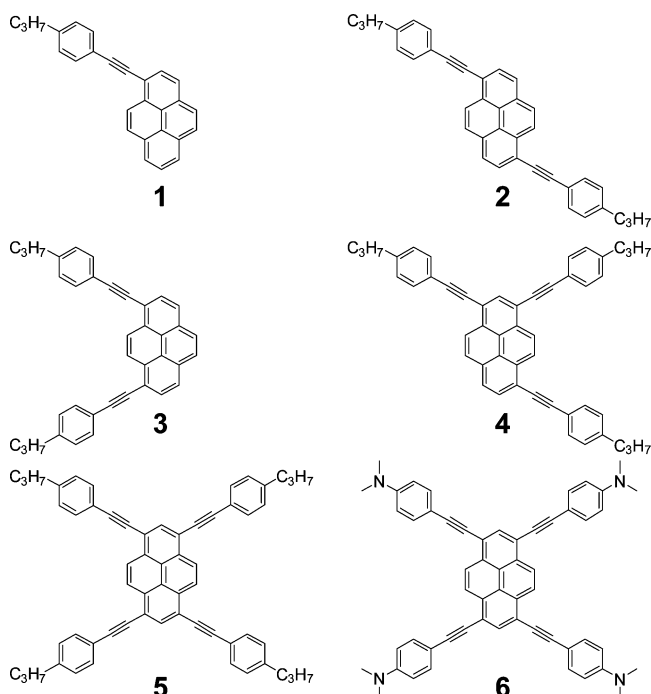
strongest ECL-active compound (6) in our previous series reported.[8a] We finally presented the DFT (density functional theory)-based theoretical calculations to achieve better understanding of the experimentally observed properties of the present series.

■ RESULTS AND DISCUSSION

Pyrene derivatives (1−5) were synthesized by the Sonogashira coupling reactions[10] of bromopyrenes (7−11) with 4-ethynylpropylbenzene as shown in Scheme 2. 1-Bromopyrene

Scheme 2. Preparation of Compounds 1−5[a]

7: X₁=Br, X₂=X₃=X₄=H

8: X₁=X₃=Br, X₂=X₄=H

9: X₁=X₄=Br, X₃=X₄=H

10: X₁=X₂=X₃=Br, X₄=H

11: X₁=X₂=X₃=X₄=Br

1: R₁=A, R₂=R₃=R₄=H

2: R₁=R₃=A, R₂=R₄=H

3: R₁=R₄=A, R₂=R₃=H

4: R₁=R₂=R₃=A, R₄=H

5: R₁=R₂=R₃=R₄=A

[a]Reagents and conditions: (a) PdCl₂(PPh₃)₂, CuI, PPh₃, Et₃N, toluene, 80 °C, 2 h.

(7), a mixture of 1,6- and 1,8-dibromopyrenes (8 and 9), 1,3,6-tribromopyrene (10), and 1,3,6,8-tetrabromopyrene (11), were prepared by the bromination of pyrene with 1−4 equiv of bromine.[11] Mono-, tris-, and tetrakis((4-propylphenyl)-ethynyl)pyrene were prepared by the ethynylation reaction.[12] To obtain 2 and 3, a mixture of 7 and 8 was reacted with A, and

the product mixture was separated by recrystallization followed by column chromatography.

Absorption and emission spectra of 1−5 in CH_2Cl_2 exhibit bathochromic shifts as the number of peripheral arms in this series increase, implying that effective extension of the conjugation occurs with the addition of phenylethynyl moieties (Figure 1a). The absorption spectra of 1−5 show a resemblance to the spectrum of pyrene in terms of band shape because there are no specific functional groups, which can cause the different excitation mode. Likewise, the emission spectra (Figure 1b) show a systematic bathochromic shift with the conjugation length increase, that is, 1 < 2 = 3 < 4 < 5, suggesting that the energy gap between the ground and excited states decreases in this order. The emission spectra of 1−5 were characterized by two defined vibrational structures observed in a typical fluorescence spectrum of pyrene. A relatively small Stokes shift of ∼10−20 nm was observed between the absorption and emission maxima of all compounds (Table 1). It reflects a small difference between the dipole moments in the ground state and Franck−Condon (FC) excited state (or locally excited (LE) state), suggesting a negligible charge transfer (CT) character in the FC excited state. Furthermore, all compounds are strongly fluorescent with high fluorescence quantum yield, which is a fundamental requirement of generating efficient ECL (Table 1.).

From the analysis of NMR spectra for 1, we observed that the 2-H pyrene peak (ortho-position to the substituent) exhibits a downfield shift from 8.0 to 8.8 ppm, which suggests delocalization of electron density from the pyrene core to the peripheral phenylethynyl moiety affecting the nearby proton most (Figure 1c). This proton even shows a greater downfield shift when the 1- and 3-positions of the pyrene core are substituted by phenylethynyl groups (in 4 and 5, for example). Additionally, the 2-H pyrene peak intensity greatly increased in 5 as 2-H and 7-H are equivalent protons in 5 (Figure 1c). The delocalization of the electron density can be understood from the frontier orbital profiles of the compounds 1−5 (Figure 3). Both HOMO and LUMO are located in pyrene core as well as in peripheral phenylethynyl groups. The delocalization of the electron density increases with increasing the peripheral arms (1→5). It is indicated that a highly conjugated network is developed in 5. Furthermore, the single-crystal X-ray structure (CCDC no. 881405) of 5 shows a nearly planar structure, which proved the presence of highly π-conjugated network in compound 5 (Figure S1, Supporting Information).

The electrochemical behavior of 1−5 and 6 was investigated by cyclic voltammetry (CV) with Bu_4NPF_6 in CH_2Cl_2 (0.1 M) on a Pt electrode, and the results show two distinctive trends as summarized in Table 1 and Figure 2. First, the electrochemical HOMO−LUMO band gap (ΔE_{gap}^{elec}) gradually decreases as the number of substitution increases in the compounds 1−5, in good agreement with energy gap trends obtained from the lowest UV/vis absorption values and DFT calculations (ΔE_{gap}^{opt} and ΔE_{gap}^{calc}, respectively, Table 1). Those results suggest that more effective conjugation in 1−5 occurs by increasing the number of peripheral arms. Second, the reversibility of the reduction and oxidation curves improves with increasing the number of the substituent group (1→5), which indicates that the extension of conjugation via a C−C triple bond alters the reversibility favorably. This is attributable to the highly conjugated network of 5, giving an extraordinary stability of both cation and anion radicals in oxidation and reduction process, respectively. For 5, we also observed that the
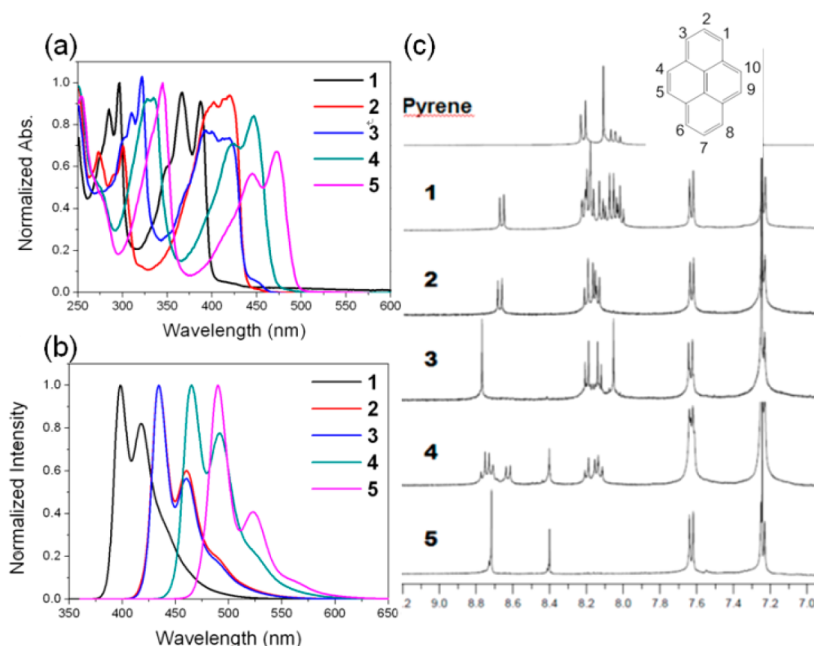
Figure 1. (a) UV/vis spectra of **1−5** in CH$_2$Cl$_2$. (b) Normalized fluorescence spectra of **1−5** in CH$_2$Cl$_2$. (c) ^{1}H NMR (CDCl$_3$, 300 MHz) spectra of pyrene and **1−5**.

Table 1. Photophysical, Electrochemical, and Theoretical DATA of 1−5

compd	1	2	3	4	5
λ_{max}^{abs} (nm)^a	387	417	419	445	472
λ_{max}^{em} (nm)	398	434	434	464	489
λ_{max}^{ECL} (nm)	550	588	582	607	612
Stokes shift (cm^{-1})	713	938	825	920	737
$\lambda_{max}^{ECL} - \lambda_{max}^{em}$ (nm)	152	154	152	147	123
Φ^b	0.78	0.99	0.82	0.89	0.87
E_{pc} (V)	−2.045	−1.961	−1.916	−1.868	−1.733
E_{pa} (V)	0.878	0.856	0.884	0.842	0.806
ΔE_{gap}^{elec} (eV)^c	2.923	2.821	2.80	2.71	2.539
ΔE_{gap}^{opt} (eV)^d	3.12	2.84	2.82	2.64	2.52
ΔE_{gap}^{calc} (eV) (DFT)	3.27	2.93	2.92	2.70	2.50

^{a}Recorded at the longest wavelengths. ^{b}Using 9,10-diphenyl anthracene (for **1−5**) in CH$_2$Cl$_2$. Φ_f = (9,10-diphenylanthracene)0.95 in EtOH.[13] ^{c}Electrochemical band gap calculated as the difference between the two peak potentials. ^{d}HOMO − LUMO gap calculated from the oneset of the UV−vis absorption.

peak separations (ΔE_{pp}) for the reversible reduction and oxidation waves are ∼90 and ∼100 mV, respectively, which are comparable to the peak separation of electrochemically reversible ferrocene, known to show Nernstian behavior under the same conditions. In comparison to **5**, compound **6** has better peak reversibility for radical cation but worse peak reversibility for the radical anion, which indicates that dimethylamine (−NMe$_2$) groups help to enhance the cation radical stability but reduce anion radical stability at the same time in **6** (Figures 2a).[9] On the other hand, **5** has good peak reversibility for both cation and anion radicals, which suggests that the replacement of a strongly electron-donating group (e.g., −NMe$_2$) with a weakly electron-donating group (e.g., *n*-propyl) in the peripheral arms helps to get better anion radical stability in **5** (Figure 2a). That is, **5** is better than **6** from the viewpoint of generating both stable cation and anion radicals simultaneously.
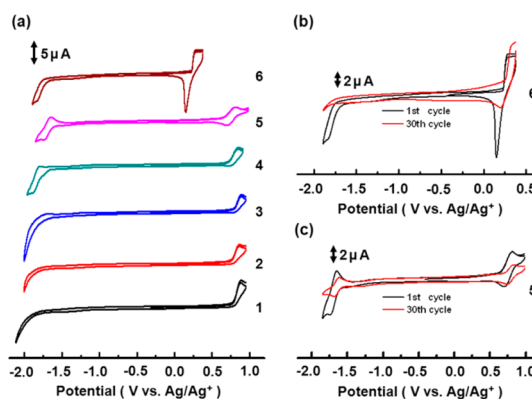

Figure 2. (a) Cyclic voltammograms of **1−6** (0.5 mM) for a Pt electrode with Bu$_4$NPF$_6$ in CH$_2$Cl$_2$ (0.1 M). Scan rate = 100 mV s^{-1}. (b) Comparison between first and 30th cycle of **6**. (c) Comparison between first and 30th cycle of **5**.

To get deeper insight into the radical stability, we have performed DFT-based theoretical calculations using the Gaussian 09 program package.[14] Figure S2 (Supporting Information) gives the spin density isosurfaces of singly occupied molecular orbitals (SOMO) of cations and anions for **1−5**. In the case of cation/anion radicals, SOMOs correspond to their HOMOs (Figures S2 and 3, Supporting Information). As shown in Figure S2 (Supporting Information), the net spin density in the SOMOs of **1**-**5** resides on pyrene core and peripheral phenylethynyl moiety. This overall electron spin density delocalization in the SOMO surfaces supports the enhanced cation (anion) radical stability at the molecular level, because electron-deficient (rich) cation (anion) radical produced after oxidation (reduction) needs immediate electron density delocalization to get thermodynamic stability at the molecular level, which can be achieved from overall well conjugated system. It can also be supported from calculated electrostatic potential (ESP) density distribution. The electrostatic potential density surfaces of the neutral molecule
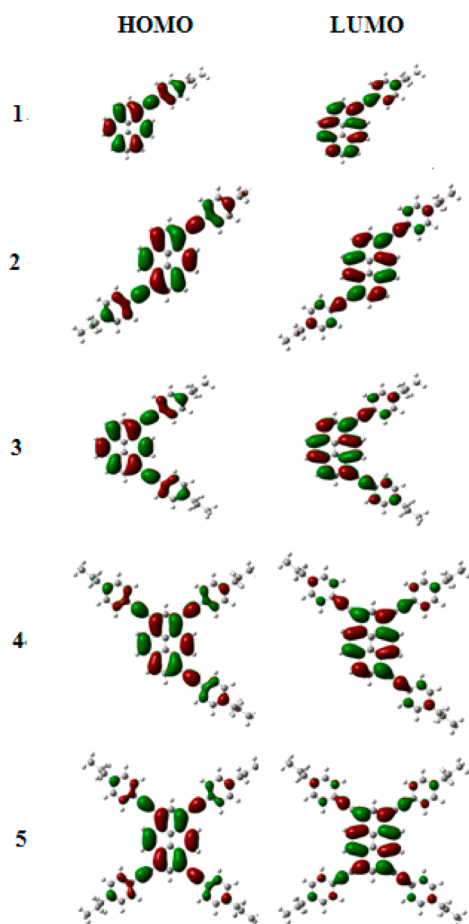
Figure 3. HOMO (left) and LUMO (right) orbital surfaces of **1−5**. Green and red correspond to the different phases of the molecular wave functions for the HOMOs and LUMOs, and the isovalue is 0.02 au.

(center), cation (left), anion (right) of **5** and **6** have been shown in Figure 4 (For **1−4**, ESP density surfaces have been
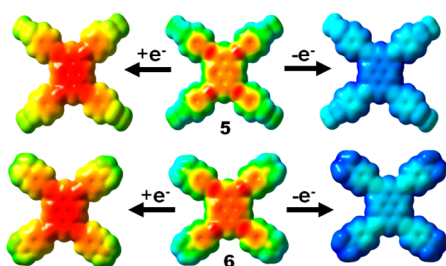

Figure 4. Top: Calculated electrostatic potential (ESP) density of **5** (middle) after adding one electron to **5** (left) and removing one electron from **5** (right). Bottom: Calculated electrostatic potential (ESP) density of **6** (middle) after adding one electron to **6** (left) and removing one electron from **6** (right). The more blue and more red, respectively, indicate more positive and more negative electrostatic potentials. Isovalue of the isosurfaces is 0.0004 au.

shown in Figure S3, Supporting Information). In Figure 4, we observed that positive charge (blue) of cation radicals as well as negative charge (red) of anion radicals reside mostly on pyrene core and phenylethynyl arms, indicating that phenylethynyl arms along with pyrene core are responsible for both cation and anion radical stability of **1−5**. It is important to note that

positive charge in **6** is more concentrated (deep blue) at the end of the peripheral donors (−NMe$_2$ groups) of cation radicals than that in **5**, which supports the better positive charge distribution due to the presence of electron donating groups (−-NMe$_2$) at the end of the peripheral donors of **6** and hence explains the better oxidation peak reversibility of **6** compared to **5** (Figure 2). The calculated non- adiabatic reduction (cation→ neutral) potential (NRP)[8a,9] for the cation radicals of **1−5** are respectively, −6.20, −5.90, −5.91, −5.72, and −5.57, implicating that cations with more number of peripheral groups are more stable than the cations with less number of peripheral groups (**1→5**), which are consistent with the analysis based on photophysical and electrochemical measurements. NRP of **6** (−4.90 eV) is larger than NRP of **5** (−5.57 eV), which also predicts higher cation radical stability of **6** than **5**. On the other hand, the calculated vertical detachment energy (VDE)[8a,9] (anion→neutral) of anion radicals **1-5** are respectively, 0.75, 1.02, 1.11, 1.34, and 1.52 eV. This implies that anion radical stability increases on going from **1** to **5**, which is also consistent with our experimental observations. It is notable that VDE of **5** is larger than **6** (1.12 eV), which predicts better anion radical stability of **5** than **6**. These results have verified that tetrakis could give a good platform to ensure stable electrochemical properties. In addition, these results clearly indicate that **5** is better than **6** with respect to simultaneous radical ion stability.

The ECL spectra were recorded in dichloromethane at 0.5 mM concentration with 0.1 M Bu$_4$NPF$_6$ as supporting electrolyte. Compound **5** shows very strong ECL emission, whereas **1−4** show very weak ECL emission (Figure 5). As
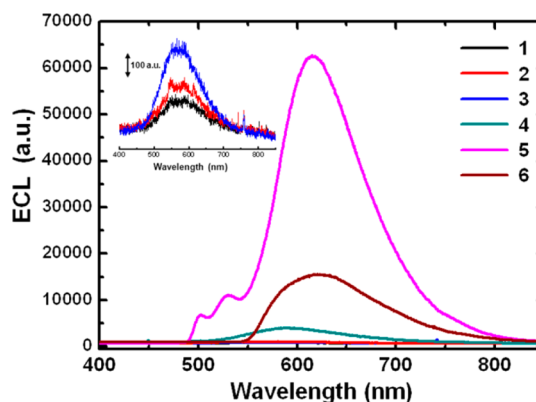
Figure 5. ECL spectra of 0.5 mM **1−6** in 0.1 M TBAPF$_6$ in CH$_2$Cl$_2$ with pulsing (10 Hz) between peak potentials for reduction and oxidation of compounds, respectively. Inset: ECL spectra of **1−3**.

shown in the spectrum of **5**, there are defined emission peaks around 490 and 610 nm. The weak ECL peaks of **5** around at 490 nm are similar to its fluorescence spectra that are mainly from the excited monomer. Pyrene derivatives are well-known to exhibit excimer emission due to its longer lifetime of the excited states.[15] Being the pyrene derivatives, **1−5** have a large possibility to form excimers when they are annihilated at the electrode surfaces during electrochemical events.[1b,16] A very strong and broad emission band (bandwidth ∼200 nm) appears in ECL of **5** at 610 nm (∼120 nm red-shifted from monomer emission). We attributed this ECL emission to the emission from the normal excimer formed by annihilation of radical ions of **5** generated electrochemically. Interestingly, the ECL intensities of **1−5** enhance remarkably as the number of

substitution increases. Although **4** and **5** have similar quantum yields, **5** shows ∼16 times enhanced ECL intensity compared to **4**. This is due to the enhanced radical stability of **5** by highly conjugated network, which is supported by photophysical and electrochemical data. The compound **5** shows even stronger ECL intensity (∼5 times) than **6** under the same experimental conditions (Figure 5). This may be mainly due to the following reasons. First, concurrent stability of both radical ions (cation and anion) of **5** provides better ECL intensity since the chances of fruitful annihilations for formation of emissive excited states between cation and anion radicals are increased. Second, the formal potential difference (ΔE^0) of **5** is larger than that of **6** (2.51 and 2.13 V, respectively), which provides comparatively greater driving force in the annihilation reaction for sufficient formation of emissive singlet excited states at a given time frame[1d,17] and consequently increases ECL efficiency. This becomes more significant when both the ionic radicals are stable. Third, upon continuous and repeated cycling (30 times), the reduction wave of **6** became irreversible at a fixed scan rate (Figure 2b) and a red thin film was formed on the electrode surface during the cycling. However, the reduction curves of **5** remained reversible even after repeated cycling (30 times), indicating a long-lived stable radical anion (Figure 2c).

■ CONCLUSIONS

In conclusion, a series of phenylethynylpyrene derivatives has been synthesized by varying phenylethynyl peripheral arms appended to the pyrene core, where a weakly electron-donating group (*n*-propyl) has been used as a substituent at the *para*-position of the phenyl group (**1**−**5**). The photophysical studies showed that **1**−**5** have large quantum yields and π-conjugated network increases with the number of peripheral arms appended to the pyrene core. The crystal structure of **5** indicated that **5** has nearly planar structure, which strengthened the notion of a well-conjugated π-network in **5**. As evidenced from the electrochemical studies, the stability of the radical ions produced electrochemically at the electrode surface enhances with the number of peripheral arms appended to the pyrene core, and both cation and anion radicals of **5** are very stable. In comparison to **6** reported previously,[8a] **5** is much better than **6** in respect of concurrent cation and anion radical stability. The replacement of strongly electron-donating group (−NMe$_2$) by a weakly electron-donating group (*n*-propyl) reduces the instability of radical anions and simultaneously balances the cation radical stability of **5**. As a result, **5** exhibited extraordinary ECL enhancement, which is ∼16 times compared to **4** and ∼5 times compared to **6**. DFT-based theoretical calculations, such as frontier molecular orbital (MO) energy and surfaces, spin density distribution (SDD) of cation/anion radicals, electrostatic potential (ESP) density distribution, nonadiabatic reduction potentials (NRP) for cation radicals, and vertical detachment energy (VDE) for anion radicals, supported the experimental observations. Our results will be useful for designing new efficient ECL materials by improving the concurrent stability of both cation and anion radicals. As **5** simultaneously provides monomer and excimer emissions, it can be used as single-dopant emitter in "small molecule" OLEDs to produce white color light by mixing a range of blue-green (monomer peak at ∼490 nm) and yellow-orange (excimer peak at ∼610 nm) wavelength lights.[18] This approach may simplify the architecture of OLED devices.

■ EXPERIMENTAL SECTION

Synthesis of Phenylethynylpyrenes. *1-(4-Propylphenylethynyl)pyrene (1).* Bromopyrene (100 mg, 0.357 mmol), PdCl$_2$(PPh$_3$)$_2$ (24 mg, 0.036 mmol), CuI (6.7 mg, 0.036 mmol), PPh$_3$ (9.3 mg, 0.036 mmol), and 1-ethynyl-4-propylbenzene (103 mg, 0.714 mmol) were added to a degassed solution of triethylamine (10 mL) and toluene (50 mL) under Ar. After the mixture was stirred at 80 °C for 5 h, the product was poured into CH$_2$Cl$_2$ (200 mL) and water (200 mL). The organic layer was separated and dried over anhydrous MgSO$_4$, and then the solvent was removed in vacuo. Column chromatography using silica gel with hexane only gave 41 mg (34%) of brown oil. Mp: 82−88 °C. IR (KBr pellet, cm^{-1}): 2200 (C≡C), 1594, 1511. ^{1}H NMR (300 MHz, CDCl$_3$): δ 8.68 (d, *J* = 9.1 Hz, 1H), 8.23−8.00 (m, 7H), 7.66 (d, *J* = 7.7 Hz, 2H), 7.26 (d, *J* = 7.9 Hz, 2H), 2.67 (t, *J* = 7.3 Hz, 2H), 1.54 (m, 2H), 0.98 (t, *J* = 7.3 Hz, 3H). ^{13}C NMR (100 MHz, CDCl$_3$): δ 143.6, 132.1, 131.8, 131.5, 131.3, 129.7, 128.9, 128.47, 128.27, 127.5, 126.4, 125.8, 125.8, 125.6, 124.8, 125.6, 95.6, 88.2, 38.3, 24.7, 14.0. HRMS (FAB-DFMS) *m/z*: [M]$^+$ calcd for C$_{27}$H$_{20}$ 344.1565, found 344.1566.

1,6-Bis(4-propylphenylethynyl)pyrene (2) and 1,8-Bis(4-propylphenylethynyl)pyrene (3). A mixture of **7** and **8** (500 mg, 1.40 mmol), PdCl$_2$(PPh$_3$)$_2$ (98 mg, 0.140 mmol), CuI (6.7 mg, 0.140 mmol), PPh$_3$ (9.3 mg, 0.140 mmol), and 1-ethynyl-4- propylbenzene (503 mg, 3.49 mmol) was added to a gassed solution of triethylamine (50 mL) and toluene (200 mL) under Ar. After being stirred at 80 °C for 3 h, the reaction mixture was poured into CH$_2$Cl$_2$ (200 mL) and water (200 mL). The organic layer was separated and dried over anhydrous MgSO$_4$, and the solvent was removed in vacuo. A 200 mL solution of toluene was added, and the yellow solid was precipitated from solution. Filtration of the solid gave 352 mg (52%) of **2** as a yellow solid. The filtrate was evaporated in vacuo, and the crude product was then subjected to column chromatograph (silica gel) with hexane only to give 204 mg (30%) of **3** as a yellow solid.

Compound **2**. Mp: 98−104 °C. IR (KBr pellet, cm^{-1}): 2200 (C≡C), 1593, 1513. ^{1}H NMR (300 MHz, CD$_2$Cl$_2$): δ 8.72 (d, *J* = 9.1 Hz, 2H), 8.24−8.20 (m, 6H), 7.66 (d, *J* = 8.2 Hz, 4H), 7.29 (d, *J* = 8.1 Hz, 4H), 2.68 (t, *J* = 7.6 Hz, 4H), 1.71 (m, 4H), 0.99 (t, *J* = 7.3 Hz, 6H). ^{13}C NMR (100 MHz, CDCl$_3$): δ 143.3, 131.8, 131.5, 130.9, 129.7, 128.5, 127.9, 126.1, 124.9, 124.1, 120.5, 118.6, 95.7, 87.8, 37.9, 24.3, 13.7. HRMS (FAB-DFMS) *m/z*: [M]$^+$ calcd for C$_{38}$H$_{30}$ 486.2348, found 486.2348.

Compound **3**. Mp: 98−104 °C. IR (KBr pellet, cm^{-1}): 2200 (C≡C), 1597, 1511. ^{1}H NMR (300 MHz, CD$_2$Cl$_2$): δ 8.80 (s, 2H), 8.22 (d, *J* = 9.8 Hz, 2H), 8.12 (s, 2H), 7.68 (d, *J* = 8.4 Hz, 4H), 7.29 (d, *J* = 7.9 Hz, 4H), 2.68 (t, *J* = 7.62 Hz, 4H), 1.71 (m, 4H), 0.99 (t, *J* = 7.3 Hz, 6H). ^{13}C NMR (100 MHz, CDCl$_3$): δ 143.7, 131.9, 131.9, 131.4, 130.0, 128.6, 128.1, 126.6, 125.2, 124.4, 120.9, 118.1, 96.1, 88.2, 38.3, 24.6, 14.1. HRMS (FAB-DFMS) *m/z*: [M]$^+$ calcd for C$_{38}$H$_{30}$ 486.2348, found 486.2347.

1,3,6-Tris(4-propylphenylethynyl)pyrene (4). 1,3,6-Tribromopyrene (100 mg, 0.229 mmol), PdCl$_2$ (PPh$_3$)$_2$ (16 mg, 0.022 mmol), CuI (5.5 mg, 0.022 mmol), PPh$_3$ (6.0 mg, 0.022 mmol), and 1-ethynyl-4-propylbenzene (165 mg, 1.15 mmol) were added to a degassed solution of triethylamine (10 mL) and toluene (50 mL) under Ar. The resulting mixture was stirred at 80 °C for 3 h. The solvent was removed under vacuum to give **3**. The crude product was then subjected to column chromatography (silica gel, hexane only) to yield **3** (52 mg, 36%) as a yellow powder. Mp: 150−190 °C. IR (KBr pellet, cm^{-1}): 2202 (C≡C), 1596, 1513. ^{1}H NMR (300 MHz, CD$_2$Cl$_2$): δ 8.75 (s, 2H), 8.69 (d, *J* = 9.1 Hz, 1H), 8.23−8.14 (m, 3H), 7.68 (m, 6H), 7.25 (d, *J* = 8.0 Hz, 6H), 2.68 (t, *J* = 7.57 Hz, 6H), 1.71−1.64 (m, 6H), 1.70 (m, 4H), 0.98 (t, *J* = 7.8 Hz, 9H). ^{13}C NMR (100 MHz, CDCl$_3$): δ 143.5, 133.2, 131.8, 131.7, 131.5, 131.1, 130.0, 128.7, 128.5, 126.1, 125.5, 124.2, 123.9, 120.5, 124.45, 120.43, 119.2, 118.51, 96.17, 95.95, 95.82, 87.9, 87.2, 38.0, 24.4, 13.8. HRMS (FAB-DFMS) *m/z*: [M]$^+$ calcd for C$_{49}$H$_{40}$ 628.3130, found 628.3130.

1,3,6,8-Tetrakis(4-propylphenylethynyl)pyrene (5). 1,3,6,8-Tetrabromopyrene (200 mg, 0.389 mmol), PdCl$_2$(PPh$_3$)$_2$ (27 mg, 0.039

mmol), CuI (7.0 mg, 0.039 mmol), PPh$_3$ (10.0 mg, 0.039 mmol), and 1-ethynyl-4-propylbenzene (280 mg, 1.95 mmol) were added to a degassed solution of triethylamine (20 mL) and toluene (80 mL) under Ar. The organic layer was separated and dried over anhydrous MgSO$_4$, and the solvent was removed in vacuo. A 200 mL solution of dichloromethane was added, and an orange solid was precipitated from solution. Filtration of the solid gave 157 mg (68%) of **5** as an orange solid. Mp: 256−276 °C. IR (KBr pellet, cm^{-1}): 2199 (C≡C), 1594, 1511. ^{1}H NMR (300 MHz, CD$_2$Cl$_2$): δ 8.78 (s, 4H), 8.43 (s, 2H), 7.67 (d, J = 7.7 Hz, 8H), 7.30 (d, J = 8.0 Hz, 8H), 2.68 (t, J = 7.55 Hz, 8H), 1.77−1.65 (m, 8H), 0.98 (t, J = 7.35 Hz, 12H). ^{13}C NMR (100 MHz, CDCl$_3$): δ 143.9, 133.8, 131.91, 131.87, 128.9, 127.0, 124.3, 120.6, 119.3, 96.5, 87.4, 38.3, 24.6, 14.1. HRMS (FAB-DFMS) m/z: [M]$^+$ calcd for C$_{60}$H$_{50}$ 770.3913, found 770.3915.

Spectroscopic Measurements. Absorption spectra were recorded on a diode array spectrophotometer with 20 μM solution of the **1−6** in CH$_2$Cl$_2$, and photoluminescence spectra were obtained with fluorescence spectrometer with a 1 cm standard quartz cell using 3 μM solution conditions in various solvents, respectively. The fluorescence quantum yields were determined by using Rhodamine 6G as the reference by the literature method.[19]

Electrochemistry and Electrogenerated Chemiluminescence Measurements. All electrochemical measurements were carried out using an electrochemical analyzer. A Pt disk (2 mm diameter) working electrode was polished with 0.3 μm alumina powder on a polishing pad and then rinsed with deionized water. Residual alumina particles were thoroughly removed by sonicating the working electrode successively in deionized water and absolute ethanol. Then, the working electrode was blown dry with a N$_2$ stream. A Pt wire and an Ag wire were used as a counter and a quasi-reference electrode, respectively. All potentials were calibrated by the addition of ferrocene as an internal standard using $E°$(Fc$^+$/Fc) = 70 mV vs Ag/Ag$^+$. ECL spectra were obtained using a monochromator and a charge-coupled device camera. A two-step potential of 10 Hz was alternatively applied with the cathodic and anodic peak potentials of the each compound during 60 s to generate ECL via radical ion annihilation. Dichloromethane solutions for ECL measurement contained 0.5 mM alkynylpyrenes at respectively and 0.1 M TBAPF$_6$ as an electrolyte.

Computational Details. The geometries of **1−5** and the geometries of their corresponding cation/anion radical species were optimized at B3LYP/6-31G(d) level of theory. No imaginary frequencies were available after vibration analysis of the optimized structures, which indicates that each of the optimized structures is at the real minimum on the potential energy surfaces (PES). The frontier molecular orbital (MO) energy and orbital surfaces, spin density distribution (SDD) surfaces, electrostatic potential (ESP) density surfaces, nonadiabatic reduction potential (NRP), and vertical electron detachment energy (VDE) were also calculated at the same level of theory using optimized geometries. The nonadiabatic reduction potential (NRP) for cation radicals and vertical electron detachment energy (VDE) for anion radicals were calculated by using the following relationships[8,9]

$$\text{NRP for cation radical} = E_{cat}(\text{cation}) - E_{cat}(\text{neutral}) \quad (1)$$

$$\text{VDE for anion radical} = E_{an}(\text{anion}) - E_{an}(\text{neutral}) \quad (2)$$

where E_{cat} (cation) and E_{an} (anion) are, respectively, energy of the cation and anion radical species. E_{cat} (neutral) and E_{an} (neutral) represent the energy of the neutral system bearing respectively the optimized structure of the cation and anion radicals. All calculations were performed using the Gaussian 09 W program package.[14]

ASSOCIATED CONTENT

Ⓢ Supporting Information

Single-crystal structure, crystal data, and atomic coordinates of **5**, NRP for the cation radicals and VDE of the anion radicals, ESP for **1−4**, absolute energies of the calculated structures, copies of ^{1}H and ^{13}C NMR spectra for all novel compounds, and atomic coordinates of compounds **1−5**. This material is available free of charge via the Internet at http://pubs.acs.org.

AUTHOR INFORMATION

Corresponding Author

*E-mail: jongskim@korea.ac.kr; jkim94@khu.ac.kr.

Author Contributions

$^\perp$These authors contributed equally to this research.

ACKNOWLEDGMENTS

REFERENCES

(1) (a) Richter, M. M. *Chem. Rev.* **2004**, *104*, 3003. (b) Miao, W. *Chem. Rev.* **2008**, *108*, 2506. (c) Grimsdale, A. C.; Chan, K. L.; Martin, R. E.; Jokisz, P. G.; Holmes, A. B. *Chem. Rev.* **2009**, *109*, 897. (d) No, K.; Lee, J. H.; Yang, S. H.; Yu, S. H.; Cho, M. H.; Kim, M. J.; Kim, J. S. *J. Org. Chem.* **2002**, *67*, 3165. (e) Lee, M. H.; Lee, S. J.; Jung, J. H.; Lim, H.; Kim, J. S. *Tetrahedron* **2007**, *48*, 12087. (f) Swamy, K. M. K.; Kwon, S. K.; Lee, H. N.; Kumar, S. M. S.; Kim, J. S.; Yoon, J. *Tetrahedron Lett.* **2007**, *48*, 8683. (g) Kim, J. S.; Kim, S. K.; Ko, J. W.; Kim, E. T.; Yu, S. H.; Cho, M. H.; Kwon, S. G.; Lee, E. H. *Talanta* **2000**, *52*, 1143. (h) Lee, S. H.; Kim, J. Y.; Ko, J.; Lee, J. Y.; Kim, J. S. *J. Org. Chem.* **2004**, *69*, 2902. (i) Kim, H. J.; Park, S. Y.; Yoon, S.; Kim, J. S. *Tetrahedron* **2008**, *64*, 1294. (j) Kim, H. J.; Lee, S. J.; Park, S. Y.; Jung, J. H.; Kim, J. S. *Adv. Mater.* **2008**, *20*, 3229.

(2) (a) Birks, J. B. *Photophysics of Aromatic Molecules*; Wiley-Interscience: London, 1970; p 354. (b) Pu, L. *Chem. Rev.* **2004**, *104*, 1687. (c) Martínez-Máñez, R.; Sancenón, F. *Chem. Rev.* **2003**, *103*, 4419. (d) Diring, S.; Camerel, F.; Donnio, B.; Dintzer, T.; Toffanin, S.; Capelli, R.; Muccini, M.; Ziessel, R. *J. Am. Chem. Soc.* **2009**, *131*, 18177.

(3) Yin, X.-B.; Dong, S.; Wang, E. *Trends Anal. Chem.* **2004**, *23*, 432.

(4) Bard, A. J., Eds. *Electrogenerated Chemiluminescence*; Marcel Dekker: New York, 2004.

(5) (a) Tang, C. W.; VanSlyke, S. A. *Appl. Phys. Lett.* **1987**, *51*, 913. (b) Huang, J.; Li, C.; Xia, Y.-J.; Zhu, X.-H.; Peng, J.; Cao, Y. *J. Org. Chem.* **2007**, *72*, 8580. (c) Huang, J.; Liu, Q.; Zhu, X.-H.; Li, A.-Y.; Li, J.-W.; Wu, S.; Peng, J.; Cao, Y.; Xia, R.; Bradley, D. D. C.; Roncali, J. *Adv, Funct. Mater.* **2009**, *19*, 2798. (d) Shen, M.; Rodríguez-López, J.; Huang, J.; Liu, Q.; Zhu, X.-H.; Bard, A. J. *J. Am. Chem. Soc.* **2010**, *132*, 13453. (e) Zhou, Y.; Kim, J. W.; Kim, M. J.; Son, W.-J.; Han, S. J.; Kim, H. N.; Han, S.; Kim, Y.; Lee, C.; Kim, S.-J.; Kim, D. H.; Kim, J.-J.; Yoon, J. *Org. Lett.* **2010**, *12*, 1272. (f) Zhou, Y.; Kim, J. W.; Nandhakumar, R.; Kim, M. J.; Cho, E.; Kim, Y. S.; Jang, Y. H.; Lee, C.; Han, S.; Kim, K. M.; Kim, J. -J.; Yoon, J. *Chem. Commun.* **2010**, *46*, 6512. (g) Zhu, X.-H.; Peng, J.; Cao, Y.; Roncali, J. *Chem. Soc. Rev.* **2011**, *40*, 3509.

(6) (a) Faulkner, L. R.; Bard, A. J. *Electroanalytical Chemistry*; Marcel Dekker: New York, 1977; Vol. 10, pp 1−95. (b) Bard, A. J.; Faulkner, L. R. *Electrochemical Methods Fundamentals and Applications*, 2nd ed.; John Wiley and Sons: New York, 2001; pp 736−745. (c) Rashidnadimi, S.; Hung, T. H.; Wong, K. T.; Bard, A. J. *J. Am. Chem. Soc.* **2008**, *130*, 634.

(7) Bard, A. J., Ed. *Electrogenerated Chemiluminescence*; Marcel Dekker: New York, 2004; Chapter 1.

(8) (a) Oh, J.-W.; Lee, Y. O.; Kim, T. H.; Ko, K. C.; Lee, J. Y.; Kim, H.; Kim, J. S. *Angew. Chem., Int. Ed.* **2009**, *48*, 2522. (b) Jiang, X.; Yang, X.; Zhao, C.; Jin, K.; Sun, L. *J. Phys. Chem. C* **2007**, *111*, 9595.

(9) Lee, Y. O.; Pradhan, T.; No, K.; Kim, J. S. *Tetrahedron* **2012**, *68*, 1704.

(10) Sonogashira, K.; Tohda, Y.; Hagihara, N. *Tetrahedron Lett.* **1975**, *16*, 4467.

(11) Grimshaw, J.; Grimsaw, J. T. *J. Chem. Soc., Perkin Trans. 1* **1972**, 1622.

(12) (a) Maeda, H.; Maeda, T.; Mizuno, K.; Fujimoto, K.; Shimizu, H.; Inouye, M. *Chem.—Eur. J.* **2006**, *12*, 824. (b) Venkataramana, G.; Sankararaman, S. *Eur. J. Org. Chem.* **2005**, 4162. (c) Yang, S.-W.; Elangovan, A.; Hwang, K.-C.; Ho, T.-I. *J. Phys. Chem. B* **2005**, *109*, 16628. (d) Kim, H. M.; Lee, Y. O.; Lim, C. S.; Kim, J. S.; Cho, B. R. *J. Org. Chem.* **2008**, *73*, 5127.

(13) Yang, W. J.; Kim, C. H.; Jeong, M. Y.; Lee, S. K.; Piao, M. J.; Jeon, S. J.; Cho, B. R. *Chem. Mater.* **2004**, *16*, 2783.

(14) Frisch, M. J.; Trucks, G. W.; Schlegel, H. B.; Scuseria, G. E.; Robb, M. A.; Cheeseman, J. R.; Scalmani, G.; Barone, V.; Mennucci, B.; Petersson, G. A.; Nakatsuji, H.; Caricato, M.; Li, X.; Hratchian, H. P.; Izmaylov, A. F.; Bloino, J.; Zheng, G.; Sonnenberg, J. L.; Hada, M.; Ehara, M.; Toyota, K.; Fukuda, R.; Hasegawa, J.; Ishida, M.; Nakajima, T.; Honda, Y.; Kitao, O.; Nakai, H.; Vreven, T.; Montgomery, J. A., Jr.; Peralta, J. E.; Ogliaro, F.; Bearpark, M.; Heyd, J. J.; Brothers, E.; Kudin, K. N.; Staroverov, V. N.; Keith, T.; Kobayashi, R.; Normand, J.; Raghavachari, K.; Rendell, A.; Burant, J. C.; Iyengar, S. S.; Tomasi, J.; Cossi, M.; Rega, N.; Millam, J. M.; Klene, M.; Knox, J. E.; Cross, J. B.; Bakken, V.; Adamo, C.; Jaramillo, J.; Gomperts, R.; Stratmann, R. E.; Yazyev, O.; Austin, A. J.; Cammi, R.; Pomelli, C.; Ochterski, J. W.; Martin, R. L.; Morokuma, K.; Zakrzewski, V. G.; Voth, G. A.; Salvador, P.; Dannenberg, J. J.; Dapprich, S.; Daniels, A. D.; Farkas, O.; Foresman, J. B.; Ortiz, J. V.; Cioslowski, J.; Fox, D. J. *Gaussian 09*, Revision B. 01; Gaussian, Inc.: Wallingford, CT, 2010.

(15) (a) Förster, T.; Seidel, H. P. *Z. Physik. Chem. NF* **1965**, *48*, 58. (b) Winnik, F. M. *Chem. Rev.* **1993**, *93*, 587.

(16) (a) Tao, X.-T; Zhang, Y.-D.; Wada, T.; Sasabe, H.; Suzuki, H.; Watanabe, T.; Miyata, S. *Adv. Mater.* **1998**, *10*, 226. (b) Wang, J.-F.; Kawabe, Y.; Shaheen, S. E.; Morrell, M. M.; Jabbour, G. E.; Lee, P. A.; Anderson, J.; Armstrong, N. R.; Kippelen, B.; Mash, E. A.; Peyghambarian, N. *Adv. Mater.* **1998**, *10*, 230.

(17) (a) Hoytink, G. J. *Discuss. Faraday Soc.* **1968**, *45*, 14. (b) Maness, K. M.; Wightman, R. M. *J. Electroanal. Chem.* **1995**, *396*, 85.

(18) (a) Andrade, B. W. D.; Forrest, S. R. *Adv. Mater.* **2004**, *16*, 1585. (b) Strukelj, M.; Jordan, R. H.; Dodabalapur, A. *J. Am. Chem. Soc.* **1996**, *118*, 1213.

(19) Crosby, G. A.; Demas, J. N. *Phys. Chem.* **1971**, *75*, 991.